Progress In Electromagnetics Research M, Vol. 97, 157–166, 2020

Wideband Low-Profile SIW Cavity-Backed Bilateral Slots Antenna for X-Band Application

Bollavathi Lokeshwar[1, *], Dorai Venkatasekhar[2], and Alapati Sudhakar[3]

Abstract—In this article, a new approach has been demonstrated for the bandwidth enlargement of a substrate integrated waveguide (SIW) cavity-backed antenna. The proposed structure employs bilateral slots, instead of unilateral slots, which is a distinct approach, in contrast to traditional cavity antennas. The proposed antenna embodies SIW cavity with a height less than $0.017\lambda_0$ and thus holds a low-profile planar geometry, while retaining lower losses and light weight. The non-resonant slot, at the bottom plate, produces two-hybrid modes (odd TE_{210} and even TE_{210}). The quality factor (Q) of these hybrid modes is greatly reduced by loading the resonant slot cut at the top metallic plate of the SIW cavity which leads to achieving a wideband response. A sample is fabricated and investigated at X-band. It is shown that the experimental results are well-matched with the simulated ones. The measured impedance bandwidth of the proposed antenna is 860 MHz, (8.6%). Moreover, it renders a maximum gain of 6.56 dBi at 9.78 GHz and 6.75 dBi at 10.35 GHz, within the operating bandwidth. The cross-polarization radiation levels of maximum −26 dB and −28 dB are obtained at the corresponding resonant frequencies, respectively.

1. INTRODUCTION

With the proliferation of wireless communication technology, the low-profile antennas with high bandwidth and gain are in huge demand at millimeter and microwave range. Printed slot antennas are being widely used in radar and satellite communications due to their excellent attributes like low-profile, simple fabrication, and conformability [1]. However, these antennas suffer from bi-directional radiation which is unwanted in many practical applications. To obliterate the backside radiation, a metallic cavity must be placed behind the radiating slot [2]. However, it substantially increases the volume of the antenna. Moreover, it makes the structure very bulky and integration very difficult with planar circuits.

Recently, a notable technology, entitled 'substrate integrated waveguide' (SIW) has drawn great attention in the microwave community due to its striking characteristics, such as less expensive fabrication, low profile, compactness, and lighter weight [3] compared to traditional waveguide. The SIW technology is smartly implemented into cavity-backed antenna structures, where sidewalls of the cavity are prepared by using four rows of metallic cylinders, inserted in a planar substrate that electrically connect the top and bottom plates [4]. Moreover, the antennas using this technology give similar advantages (unidirectional radiation pattern and high gain) as that of conventional cavity-backed antennas (CBSAs).

The first low-profile slot antenna, based on SIW technology, is discussed in [5], where a low height (0.5 mm) SIW cavity is used, in the place of a bulky metallic cavity to achieve unidirectional radiation pattern. However, it possesses narrow bandwidth, due to low height substrate. In general, the SIW

Received 30 August 2020, Accepted 30 September 2020, Scheduled 16 October 2020
* Corresponding author: Bollavathi Lokeshwar (lokesh5701@gmail.com).
[1] Department of ECE, Annamalai University, Annamalainagar, India. [2] Department of IT, Annamalai University, Annamalainagar, India. [3] Department of ECE, R.V.R & J.C College of Engineering, Guntur, India.

cavity quality factor (Q) is increased due to the thin substrate. As a result, it decisively influence the bandwidth. Thus, designing SIW CBSAs to obtain wide impedance bandwidth with low height substrate remains an arduous task to the designers.

In the literature, a variety of methods have been investigated to address the narrow bandwidth of the SIW CBSAs, since the past decade. The first method is reported in [6], in which two hybrid modes (combinations of TE_{120}, TE_{210}) of the SIW cavity are used to improve the bandwidth up to 6.3%. The second method is discussed in [7], in which Q of the SIW cavity is curtailed by partially removing the substrate. As a result, impedance bandwidth is enhanced. However, it is a difficult job to detach the substrate during fabrication. The third method of enhancing the bandwidth is reported in [8], in which single via-hole is inserted, just above the slot to enlarge the bandwidth. However, betterment in the bandwidth does not surmount 90 MHz (3.7%) in this work. The fourth method is presented in [9], in which bandwidth is enlarged by using a multi-layer structure, but it increases the height of the antenna and complexity in the design.

The fifth method is presented in [10], in which the offset feeding technique is used, instead of center feeding to enhance the bandwidth. It exhibits a fractional bandwidth of 4.2%. In [11], perturbed SIW cavity is used, in the place of regular SIW cavity to increase the bandwidth. Square SIW cavity is perturbed by the corner cut to couple the hybrid modes. In [12], wideband SIW CBSA is presented with the same perturbation approach, as discussed in [11]. However, instead of single corner cut, two circular corner cuts are perturbed to broaden the bandwidth. In [13], instead of embedding one via-hole, above the slot, as presented in [8], two via holes are inserted, precisely near the two tilted slots to extend the antenna bandwidth considerably. In [14], stacked cavities are used to increase the bandwidth, in SIW cavity-backed antennas.

In this study, a novel approach wideband response of cavity-backed antenna with low height (0.5 mm) dielectric substrate is presented. This method consigns the bilateral slots, instead of unilateral slots, which is a more diverse approach than other methods, presented in [6–14]. The bilateral slots cause the quality factor (Q) of the SIW cavity to decrease. Consequently, two closely spaced hybrid modes are generated at 9.76 GHz and 10.36 GHz. The designed antenna is analyzed by the electromagnetic full-wave simulator. The simulated impedance bandwidth is 860 MHz from 9.57 GHz to 10.43 GHz with a stable gain. The fabricated prototype is then tested to compare with simulated counterpart. It will be shown that the experimental results match very well with the simulated counterparts.

2. ANTENNA CONFIGURATION

The schematic of the proposed low-profile wideband bilateral slots antenna, based on SIW cavity and its perspective view, is shown in Figure 1. The proposed design is composed of a SIW cavity and two transversal slots. Moreover, to facilitate the planar configuration, a single 50 Ω grounded coplanar waveguide (GCPW) elongated by micro-strip line is employed to stimulate the proposed antenna. The entire SIW cavity of the proposed design is realized on a single dielectric substrate, whose four side walls are prepared by metallic posts arranged uniformly. These metallic posts connect the top and bottom copper layers to each other, which help to realize the other two walls of the cavity. The post diameter 'd' and distance between adjacent via-holes (pitch) 'p' need to satisfy the indispensable guidelines ($p \leq 2d$ and $d \leq 0.1\lambda_0$) to reduce leakage losses between the consecutive vias. The preliminary dimensions of the planar cavity have been calculated by using the following formulae [15].

$$f_{mn0} = \frac{c}{2\sqrt{\varepsilon}_r}\sqrt{\left(\frac{m}{L_{eff}}\right)^2 + \left(\frac{n}{W_{eff}}\right)^2} \tag{1}$$

$$L_{eff}(or\, W_{eff}) = L_c(or\, W_c) - \frac{d^2}{0.95 * p} \tag{2}$$

where m and n are half-wave field variations in x and y directions, respectively; c and ε_r refer to the light velocity in free space and dielectric constant, respectively; W_c is the SIW cavity width; L_c is the SIW cavity length; d is the cylinder diameter; p is the pitch.

Two rectangle slots with unequal lengths are placed above the centerline of the cavity. A long slot of dimension ($L_{s1} \times W_{s1}$) is imprinted at the bottom cladding of the cavity, at a distance d_1, from

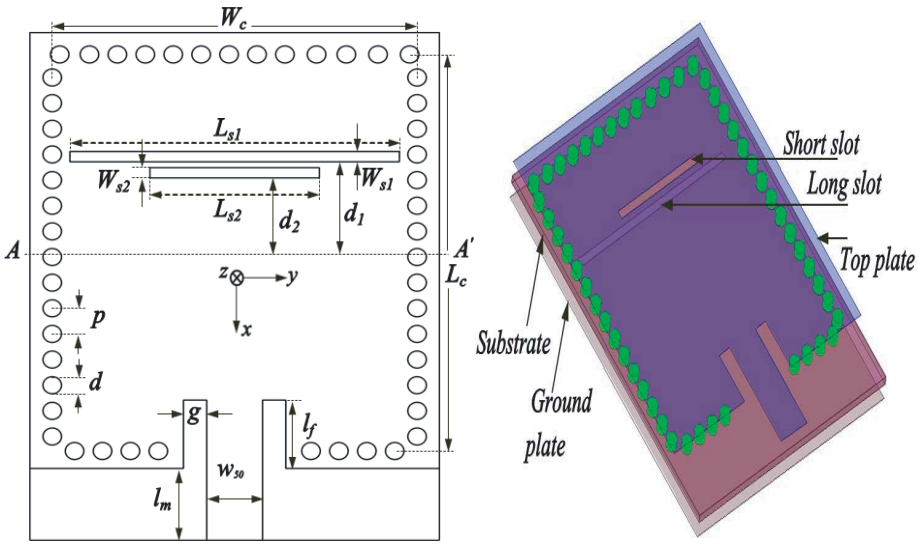

Figure 1. (a) Schematic of the designed wideband antenna and (b) 3D view. [$W_c = 19.6$, $L_c = 23.2$, $L_{s1} = 17.7$, $W_{s1} = 0.6$, $d_1 = 5.34$, $L_{s2} = 9.1$, $W_{s2} = 0.6$, $d_2 = 4.4$, $p = 1.5$, $d = 1$, $w_{50} = 3$, $l_f = 4$, $g = 1.25$, $l_m = 4.2$, $h = 0.5$]. (Units: mm).

centerline AA'. Similarly, a short slot, having the same width, as that of the long slot is engraved on the top cladding and positioned at a distance of d_2 from AA'. Optimally, offset (a gap between two slots) value is chosen as 0.34 mm (d_1–d_2–W_{s2}) to achieve better impedance matching within the operating bandwidth.

3. PRINCIPLE OF OPERATION

3.1. Antenna without Short Slot

To comprehend the behavior of the short rectangle slot on bandwidth enlargement, the unloaded SIW cavity and loaded SIW cavity with a long rectangle slot are described with the aid of input resistance (real (Z_{11})) plot as illustrated in Figure 2. It is noted that peaks of real (Z_{11}) plot are used to recognize the cavity modes. The size of the SIW cavity is optimized in such a manner to operate in X-band. When the SIW cavity alone is stimulated by GCPW feed element, and the dominant mode (TE_{110}) at 7.1 GHz and TE_{210} mode at 10.3 GHz are generated. The electric field distribution of the TE_{110} and TE_{210} modes extricated by HFSS solver is shown in Figure 3.

The aforementioned cavity modes get excited by etching the long rectangle slot (non-resonant slot) at the ground plate of the cavity. As a result, the fundamental TE_{110} mode shifts downward from 7.1 GHz to 6.4 GHz. The mode obtained at 6.4 GHz is known as half-TE_{110}, since its electric field has large magnitude difference at two sides of the long slot and gradually reduces from the center, towards the cavity edges. Other than the half TE_{110} mode, a new couple of hybrid modes (odd TE_{210} and even TE_{210}) are generated in the close frequency range, at 10.2 GHz and 10.4 GHz due to perturbations in TE_{210} mode. Figure 4 depicts the electric field distributions of the cavity, with a long transversal slot.

3.2. Antenna with Short Slot

Due to the strong loading effect, the quality factor (Q) of the cavity is significantly reduced. Thus, the wideband response is obtained in the desired operating band. It can be indubitably explained by the same input resistance (real Z_{11}) plot, as shown in Figure 2. It is evident that the half TE_{110} mode is almost unperturbed due to the short slot (resonant slot) which is inserted on the top plate of the cavity.

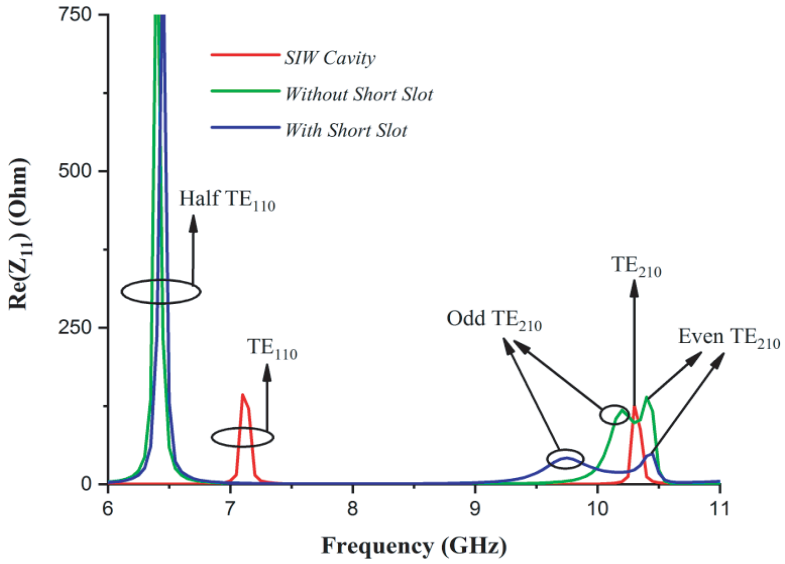

Figure 2. Input resistance (Real Z_{11}) plot.

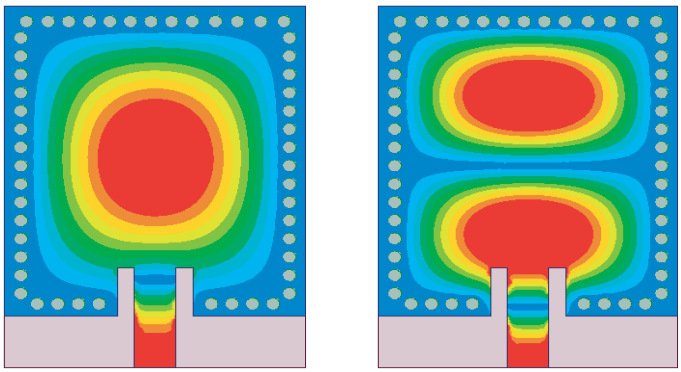

Figure 3. Electric field distributions of the unloaded SIW cavity. (a) 7.1 GHz. (b)10.3 GHz.

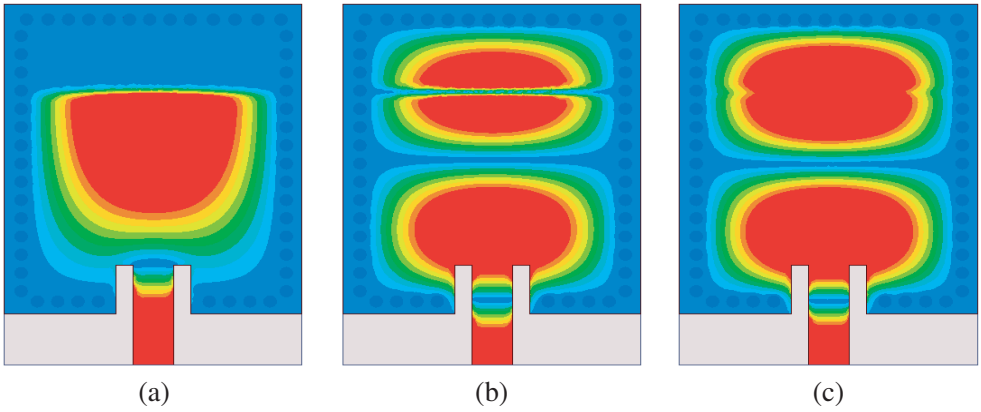

Figure 4. Electric field distributions of the loaded SIW cavity with long slot. (a) 6.4 GHz. (b) 10.2 GHz. (c) 10.4 GHz.

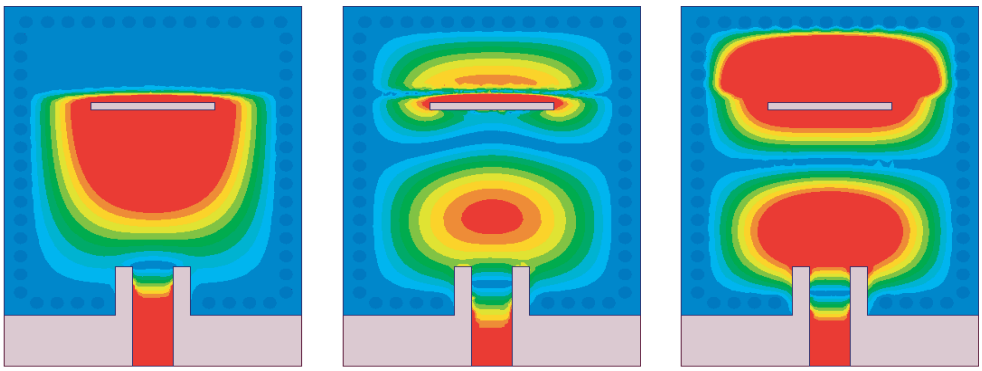

(a) (b) (c)

Figure 5. Electric field distributions for the bilateral slots. (a) 6.45 GHz. (b) 9.75 GHz. (c) 10.45 GHz.

The same can be observed in Figure 5(a). Moreover, this half TE_{110} mode is not involved in enhancing the bandwidth.

With the introduction of a short slot, the impedance matching of the antenna is observed more. It can be observed that the resonance of the odd TE_{210} mode has been reduced greatly due to the incorporation of the resonant slot. The original odd TE_{210} mode at 10.2 GHz is moved to 9.75 GHz, which leads to reducing the quality factor (Q) value of the cavity. Similarly, the original even TE_{210} mode is slightly shifted upward from 10.4 GHz to 10.45 GHz. Consequently, the even TE_{210} mode quality factor (Q) is also decreased. Thus, it can be said that the odd TE_{210} and even TE_{210} modes contribute significantly to bandwidth enhancement. However, even TE_{210} mode at 10.45 GHz is not within the obtained bandwidth range (9.57 GHz to 10.43 GHz). Figures 5(b) and (c) represent the electric field distributions of the odd TE_{210} and even TE_{210} modes, respectively. Therefore, the input impedance (Z_{11}) of the proposed design strongly depends on the appropriate selection of short slot, above the AA' line and inset of the feed line.

In order to examine the radiation characteristics of the proposed antenna with more insight, the surface current density of the proposed wideband antenna at different resonances is depicted in Figure 6. It is evident that the Q of the hybrid mode at 9.76 GHz is less than that of the hybrid mode at 10.36 GHz, which can be noticed by comparing Figures 6(a) and (b). Figure 6(a) depicts that, at 9.76 GHz, the surface current becomes strong in the overlap portion of the two slots and weak below the resonant slot. At this frequency, the magnitude of the electric field at two sides of the non-resonant slot is out of phase, which consequently helps the slot to radiate electromagnetic wave into free space. As can be

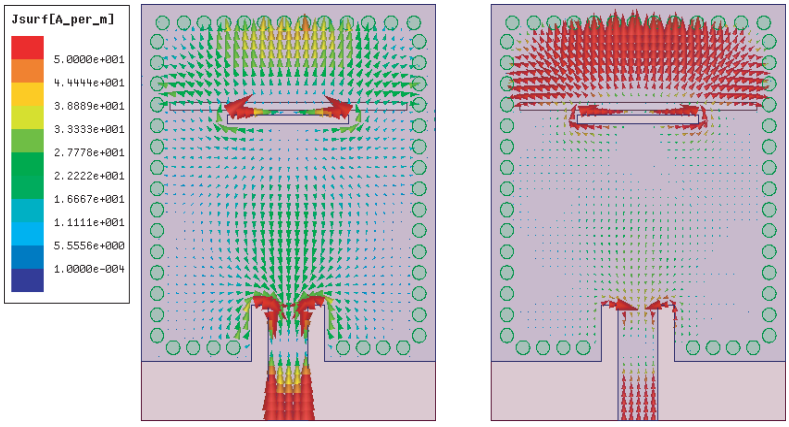

(a) (b)

Figure 6. Surface current distribution vector at (a) 9.76 GHz, (b) 10.36 GHz.

seen, long transversal slot plays a vital role behind the radiation at 9.76 GHz.

Similarly, at 10.36 GHz, the surface current density is predominantly concentrated, above the non-resonant slot, on the upper half of the cavity, meanwhile minimal amount of field prevail in the lower half as shown in Figure 6(b). At this frequency also, the electric field strength has opposite phases, at both sides of the slot, which can make the slot to radiate into air.

4. PARAMETRIC STUDY

To examine the influence of various key parameters on the frequency characteristics, a parametric analysis is explicated for further study. Key parameters of the proposed structure are symbolically indicated in Figure 1. The alterations of two resonances on S_{11} of the proposed design with the slot widths (W_{s1}, W_{s2}) and positions (d_1, d_2) are described in this section. In the course of parametric analysis, observation parameter is only changed, and rest of the optimized parameters remains unchanged. This procedure promotes the flexibility and practical utility in the design of antennas.

The effects of the slot positions (d_1, d_2) from AA' line (centerline of the cavity) have been elaborated in Figure 7. By shifting the positions of either d_1 or d_2, the overlap region between the two slots can be changed. As shown in Figure 7(a), the variation in the value of d_1 from 4.94 mm to 5.86 mm leads to perturbation in the TE_{210} mode. As a result, at optimum $d_1 = 5.34$ mm, the impedance matching is significantly improved, and the corresponding bandwidth is also greatly increased. Likewise, if the short slot is shifted away from the centerline (AA'), as indicated in Figure 7(b), the impedance bandwidth is improved due to the shift of odd TE_{210} mode. Hence, at optimum $d_2 = 4.4$ mm, maximum bandwidth is obtained with good impedance matching.

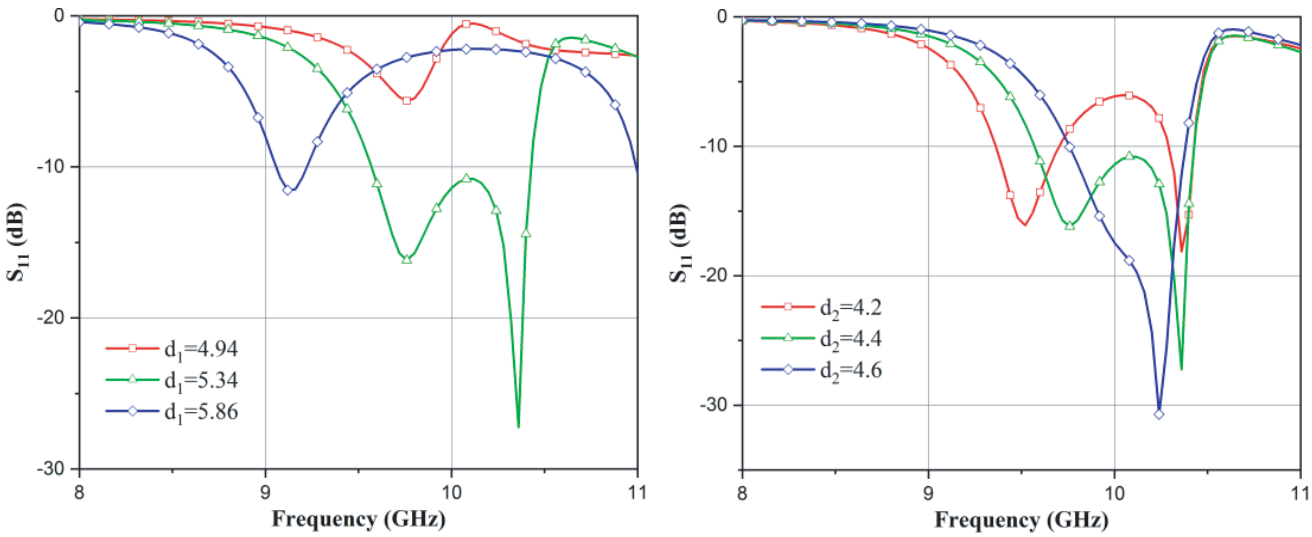

Figure 7. Reflection coefficient (S_{11}) variations with different values of (a) d_1, (b) d_2.

The influence of slot widths W_{s1} and W_{s2} on impedance bandwidth is plotted in Figure 8. In Figure 8(a), as the long slot width W_{s1} increases, the lower resonances increase, and the upper resonances are almost unchanged. Thus, the lower frequency region of operating bandwidth is correspondingly increased while the upper-frequency region remains constant. Likewise, width W_{s2} of short slot has no impact on the upper resonance. However, the lower frequencies are lowered slowly, by increasing the W_{s2}, as shown in Figure 8(b). As a result, the corresponding lower resonant frequency boundary of bandwidth is reduced.

It is concluded from the parametric analysis that by individually switching the parameters d_2, W_{s1}, W_{s2} of the proposed antenna, the lower frequency can be tuned independently which puts forward the design to have more freedom on the impedance bandwidth, for the antenna designer.

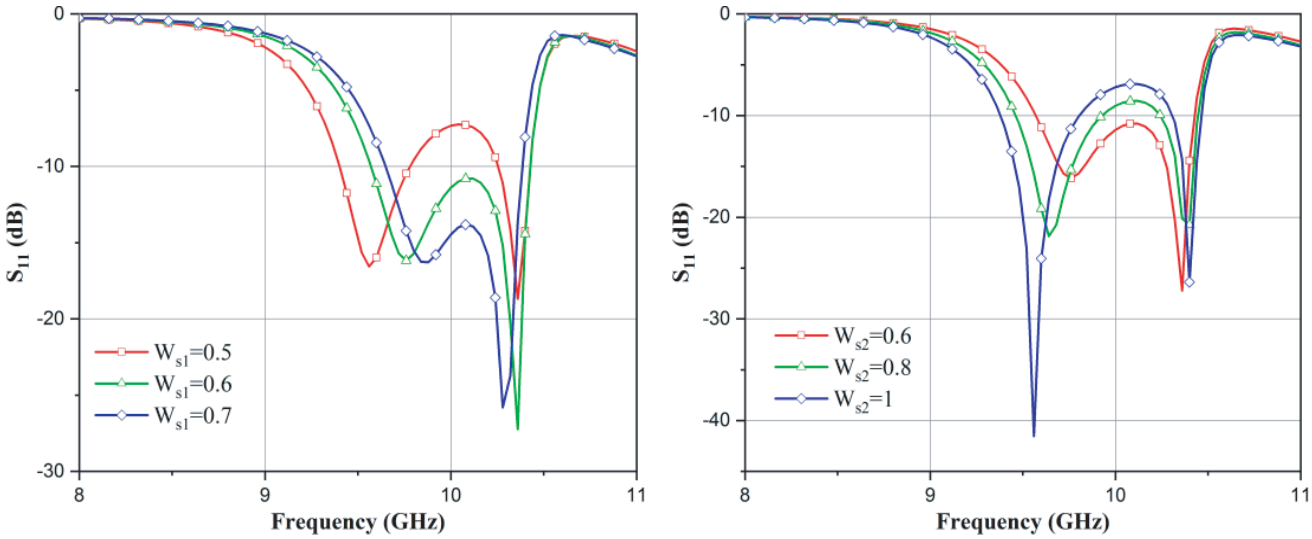

Figure 8. Reflection coefficient (S_{11}) variations by slot width. (a) W_{s1}. (b) W_{s2}.

5. RESULTS AND DISCUSSION

To corroborate the simulation performance (reflection coefficient, gain, and radiation pattern) extracted by using Ansoft HFSS, the designed SIW cavity-backed wideband bilateral slots antenna is fabricated on an RT/Duroid 5880 substrate whose relative permittivity (ε_r) is 2.2, and thickness (h) is 0.5 mm. Figure 9 displays the top and bottom photographs of the fabricated sample. Figure 10 represents both the simulated and measured responses of reflection coefficient (S_{11}) of the proposed antenna. It can be substantiated from the figure that the measured S_{11} are almost close to simulated ones. However, there is a small discrepancy, observed in the impedance matching and frequency shift, between the simulated and measured results which may be due to fabrication imperfections and soldering errors.

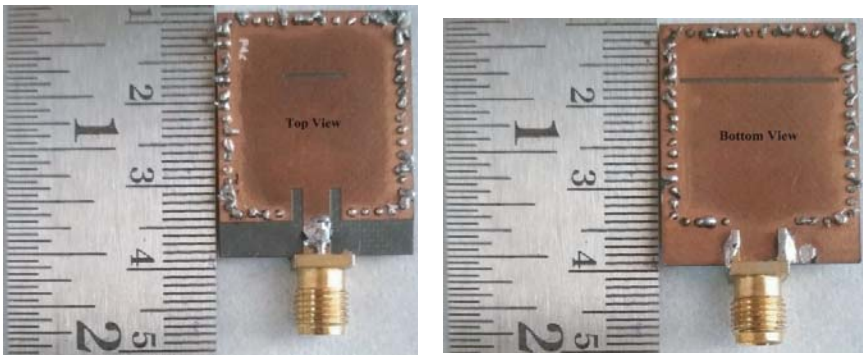

Figure 9. Photographs of the proposed wideband antenna. (a) Top view. (b) Bottom view.

The simulated S_{11} exhibits the impedance bandwidth 860 MHz (8.6%), covering from 9.57 GHz to 10.43 GHz, with the measured one from 9.59 GHz to 10.45 GHz (8.6%). Moreover, Figure 10 also illustrates the simulated and measured gain results in the boresight direction. It may be observed that the simulated gain is stable and exhibits peak gains of 6.35 dBi and 6.56 dBi at 9.76 GHz and 10.36 GHz, respectively. The measured peak gains of 6.56 dBi, at 9.78 GHz and 6.75 dBi, at 10.35 GHz have been

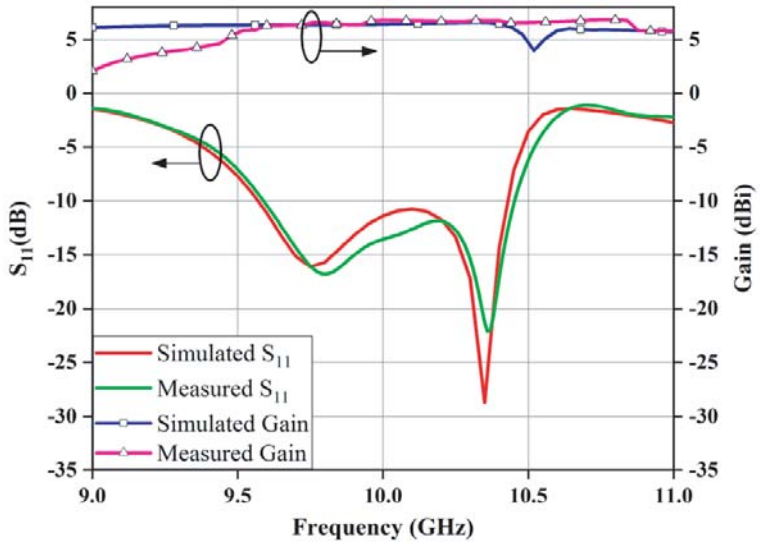

Figure 10. Simulated and measured S_{11} and gain of the proposed wideband antenna.

achieved, which are near the simulated counterpart.

The simulated normalized co-pol and cross-pol radiation patterns of the proposed design in two cut-planes ($\phi = 0°$ and $\phi = 90°$), at two different frequencies are shown in Figure 11. At positive radiating direction ($90° \leq \theta \leq 270°$), in both the planes, the simulated cross-polarization levels of the proposed antenna are below -25 dB, at both the resonances. Figure 11 also includes the measured radiation patterns. It is found from the measured results that the peak cross-polarization radiation values in the XZ- and YZ-planes are -25 dB and -26 dB, respectively, at lower resonance. At 10.36 GHz, the peak cross-pol levels are -28 dB and -20 dB in the XZ-plane and YZ-plane, respectively.

It can be seen that the major lobe is tilted, a little from the boresight direction, in XZ-plane, at lower and higher frequencies. On the other hand, the main lobe is evidently at boresight direction ($\theta = 180°$) in YZ-plane. It is noted that the radiation patterns in two cut-planes are unidirectional due to cavity-backing geometry. The half-power beamwidths of the co-polarized pattern in XZ- and YZ-planes are about 111.5° and 73.5°, respectively, in the lower band. Similarly, they are 115° and

Table 1. Assessment of proposed antenna with previously reported antennas.

Properties	f_r (GHz)	Impedance bandwidth		Gain (dBi)	ε_r	Cavity Size (λ_0^3)
		(MHz)	FBW (%)			
Proposed work	10	860	8.6	6.75	2.2	$0.77 \times 0.65 \times 0.02$
[6]	10	630	6.3	6	2.2	$0.41 \times 0.59 \times 0.02$
[7]	2.45	53	2.16	NM	4.4	$0.37 \times 0.45 \times 0.01$
[8]	2.45	82	3.34	5.8	2.2	$0.46 \times 0.52 \times 0.01$
[10]*	10.2	430	4.2	5.6	2.2	$0.51 \times 0.57 \times 0.03$
[11]	13.2	220	1.65	5.2	2.2	$0.78 \times 0.78 \times 0.03$
[12]	14	800	5.7	6.4	2.2	$0.84 \times 0.84 \times 0.03$
[13]	5.8	300	5.2	7.15	3.55	$0.73 \times 0.39 \times 0.03$
[14]	4	150	3.75	4.42	2.5	$0.50 \times 0.58 \times 0.02$

* — simulated results; f_r — operating frequency; NM — not mentioned.

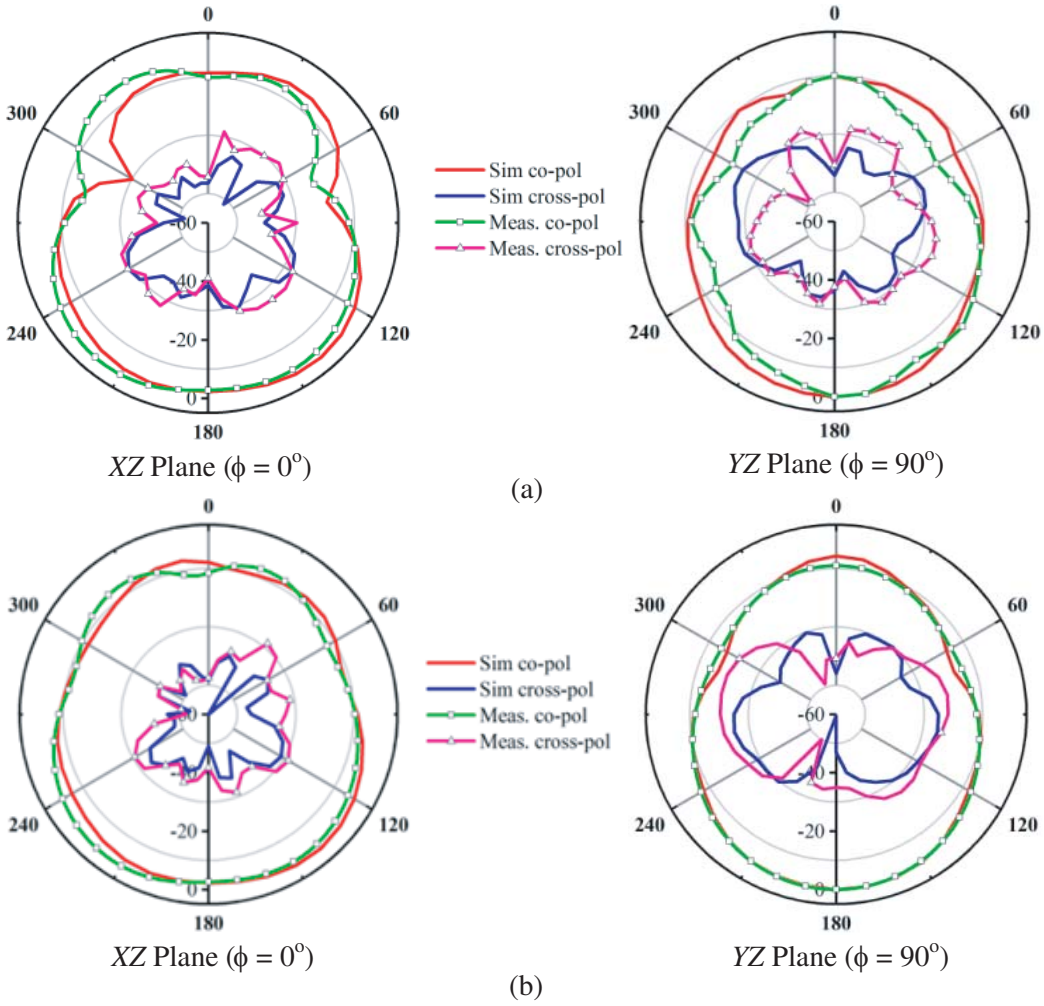

Figure 11. Simulated and measured normalized radiation patterns at (a) 9.78 GHz, (b) 10.35 GHz.

77° at $\phi = 0°$ and $\phi = 90°$ planes, respectively, in the upper band. To accentuate the essence of the proposed work, the performance of the proposed wideband antenna with previously reported antennas is listed in Table 1. It may be noted that the proposed design increases the bandwidth considerably, with enough gain.

6. CONCLUSION

An extensive study of a novel wideband antenna is discussed in this paper. In the proposed design, bilateral slots are incorporated, above the center portion of the SIW cavity. Consequently, the quality factor of the hybrid cavity modes (odd TE_{210}, even TE_{210}) is decreased, which helps to widen the bandwidth of the antenna significantly. The fabricated prototype has been tested to verify antenna performance. The experimental results ascertain that the proposed antenna produces a wideband response with an 8.6% fractional bandwidth. The antenna also consigns a flat gain, in the band of interest and exhibits low cross-polarization level at all the resonant frequencies. The proposed geometry also imparts other benefits such as low profile, light weight, cost-effective fabrication, and easy integration with planar configurations. Finally, with a wideband response, the proposed structure is a desirable candidate for X-band applications. Further, the proposed design can be readily extended to SIW array structures or a higher number of cavities.

REFERENCES

1. Lee, Y. C. and J. S. Sun, "Compact printed slot antennas for wireless dual-and multi-band operations," *Progress In Electromagnetics Research*, Vol. 88, 289–305, 2008.
2. Zhou, S. G., G. L. Huang, and T. H. Chio, "A low-profile wideband cavity-backed bowtie antenna," *Microw. Opt. Techno. Lett.*, Vol. 55, No. 6, 1422–1426, 2013.
3. Deslandes, D. and K. Wu, "Accurate modeling wave mechanisms and design considerations of substrate integrated waveguide," *IEEE Trans. Microw. Theory Tech.*, Vol. 54, No. 6, 2516–2526, 2006.
4. Luo, G. Q., T. Y. Wang, and X. H. Zhang, "Review of low profile substrate integrated waveguide cavity backed antennas," *Int. J. Antennas Propag.*, 746920, 2013.
5. Luo, G. Q., Z. F. Hu, L. X. Dong, and L. L. Sun, "Planar slot antenna backed by substrate integrated waveguide cavity," *IEEE Antennas Wirel. Propag. Lett.*, Vol. 7, No. 8, 236–239, Aug. 2008.
6. Luo, G. Q., Z. F. Hu, W. J. Li, X. H. Zhang, L. L. Sun, and J. F. Zheng, "Bandwidth-enhanced low-profile cavity-backed slot antenna by using hybrid SIW cavity modes," *IEEE Trans. Antennas Propag.*, Vol. 60, No. 4, 1698–1704, 2012.
7. Yun, S., D. Kim, and S. Nam, "Bandwidth and efficiency enhancement of cavity-backed slot antenna using a substrate removal," *IEEE Antennas Wirel. Propag. Lett.*, Vol. 11, 1458–1461, 2012.
8. Yun, S., D. Kim, and S. Nam, "Bandwidth enhancement of cavity-backed slot antenna using a via-hole above the slot," *IEEE Antennas Wirel. Propag. Lett.*, Vol. 11, 1092–1095, 2012.
9. Yang, W. and J. Zhou, "Wideband low-profile substrate integrated waveguide cavity-backed E-shaped patch antenna," *IEEE Antennas Wirel. Propag. Lett.*, Vol. 12, 143–146, 2013.
10. Mukherjee, S., A. Biswas, and K. V. Srivastava, "Bandwidth enhancement of substrate integrated waveguide cavity backed slot antenna by offset feeding technique," *IEEE Applied Electromagnetics Conf. (AEMC)*, Dec. 2013.
11. Baghernia, E. and M. H. Neshati, "Development of a broadband substrate integrated waveguide cavity backed slot antenna using perturbation technique," *Appl. Comput. Electro. Soc. J.*, Vol. 29, No. 11, 847–855, 2014.
12. Heydarzadeh, F. and M. H. Neshati, "Design and development a wideband SIW based cavity-backed slot antenna using two symmetrical circular corner perturbations," *Int. J. RF Microw. Comput. Aided Eng.*, Vol. 28, No. 9, e21552, 2018.
13. Chaturvedi, D., "SIW cavity-backed 24o inclined-slots antenna for ISM band application," *Int. J. RF Microw. Comput. Aided Eng.*, Vol. 30, No. 5, e22160, 2020.
14. Ali, H. A., E. Massoni, L. Silvestri, M. Bozzi, L. Perregrini, and A. Gharsallah, "Increasing the bandwidth of cavity-backed SIW antennas by using stacked cavities," *Int. J. Microw. and Wireless Tech.*, Vol. 10, No. 8, 942–947, 2018.
15. Lokeshwar, B., D. Venkatasekhar, and A. Sudhakar, "Dual-band low profile SIW cavity-backed antenna by using bilateral slots," *Progress In Electromagnetics Research C*, Vol. 100, 263–273, 2020.